JOURNAL OF VIROLOGY, Jan. 1995, p. 131–140 Vol. 69, No. 1
0022-538X/95/$04.00+0

Efficient System of Homologous RNA Recombination in Brome Mosaic Virus: Sequence and Structure Requirements and Accuracy of Crossovers

PETER D. NAGY AND JOZEF J. BUJARSKI*

Plant Molecular Biology Center and Department of Biological Sciences, Northern Illinois University, De Kalb, Illinois 60115

Received 1 July 1994/Accepted 23 September 1994

Brome mosaic virus (BMV), a tripartite positive-stranded RNA virus of plants engineered to support intersegment RNA recombination, was used for the determination of sequence and structural requirements of homologous crossovers. A 60-nucleotide (nt) sequence, common between wild-type RNA2 and mutant RNA3, supported efficient repair (90%) of a modified 3′ noncoding region in the RNA3 segment by homologous recombination with wild-type RNA2 3′ noncoding sequences. Deletions within this sequence in RNA3 demonstrated that a nucleotide identity as short as 15 nt can support efficient homologous recombination events, while shorter (5-nt) sequence identity resulted in reduced recombination frequency (5%) within this region. Three or more mismatches within a downstream portion of the common 60-nt RNA3 sequence affected both the incidence of recombination and the distribution of crossover sites, suggesting that besides the length, the extent of sequence identity between two recombining BMV RNAs is an important factor in homologous recombination. Site-directed mutagenesis of the common sequence in RNA3 did not reveal a clear correlation between the stability of predicted secondary structures and recombination activity. This indicates that homologous recombination does not require similar secondary structures between two recombining RNAs at the sites of crossovers. Nearly 20% of homologous recombinants were imprecise (aberrant), containing either nucleotide mismatches, small deletions, or small insertions within the region of crossovers. This implies that homologous RNA recombination is not as accurate as proposed previously. Our results provide experimental evidence that the requirements and thus the mechanism of homologous recombination in BMV differ from those of previously described heteroduplex-mediated nonhomologous recombination (P. D. Nagy and J. J. Bujarski, Proc. Natl. Acad. Sci. USA 90:6390–6394, 1993).

Natural sequence rearrangements in several animal and plant RNA virus groups have been observed (15, 33). Sequence comparisons have also revealed the modular nature of the assembly of RNA viral genomes (15, 17, 19, 59). All these data emphasize the importance of RNA recombination for increasing variability and facilitating evolution in RNA viruses (15, 18, 28, 33, 52).

To date, RNA recombination has been demonstrated experimentally in animal viruses, including picornaviruses (28), coronaviruses (33), alphaviruses (57), orthomyxoviruses (7), and nodaviruses (34); in plant viruses, including bromoviruses (4, 10, 47), carmoviruses (13), tombusviruses (58), tobamoviruses (6, 44), and alfalfa mosaic virus (54); and in bacteriophages (39, 40). These studies reveal that RNA recombination can be either precise (homologous) or imprecise (nonhomologous), involving homologous or heterologous sequences, respectively, at junction sites.

Homologous recombination is the most common type of RNA recombination. It is thought to utilize a replicase-mediated copy-choice mechanism (11, 24, 33). In picornaviruses, crossovers occurred between mutants of the same virus strain or between different virus strains within regions containing several hundred homologous nucleotides (28). In coronaviruses, homologous recombination took place between genomic RNAs of different strains or mutants, between subgenomic and genomic RNAs, and between defective interfering and genomic RNAs (30, 35, 55). Homologous recombination has also occurred within a large region of a 3′ mutated replicase gene of bacteriophage Qβ and wild-type (wt) Qβ replicase mRNA expressed from a plasmid (40). Because homologous crossovers occurred between identical or highly homologous sequences, the exact recombination sites were not determined unambiguously in the studies mentioned above. Thus, the structure and/or sequence requirements for homologous RNA recombination have been difficult to characterize. Romanova et al. (48) and Tolskaya et al. (53) suggested that two parental picornavirus positive-sense RNA templates could form a local heteroduplex at regions of self-complementarity, facilitating the generation of homologous recombinants. Alternatively, a supporting negative-sense RNA might help to bring the two parental positive-sense RNA templates together (31). For coronaviruses, similar secondary structures between parental molecules have been proposed to facilitate homologous recombination (35). In some cases, however, short sequence homologies between parental templates were proposed to facilitate nonhomologous recombination events (8, 58). These models have not been experimentally confirmed.

Brome mosaic virus (BMV) is a tripartite, single-stranded RNA virus of plants. The genomic RNA components of BMV contain approximately 200 nucleotides (nt) of homologous 3′ noncoding sequence (2). The 3′ portion of this region can form a tRNA-like conformation which is involved in the initiation of minus-strand synthesis (for a review, see reference 36). Most of the recombination experiments with BMV have utilized RNA3 mutants since this is the only RNA segment which does not provide indispensable *trans*-acting RNA replication factors (1). Intersegment genetic recombination in BMV was first ob-

* Corresponding author.

served when a viable BMV RNA3 mutant (designated m4) containing a deletion within the 3′ noncoding sequence was repaired because of crossovers with wt RNAs 1 or 2 (10). Other homologous and nonhomologous BMV recombinants have since been isolated from *Chenopodium hybridum*, a local lesion host (37, 47), and from barley, a systemic host (9). Mutants incapable of replication recombined with replication-competent wt RNAs (22, 38, 45). A replicase-driven template switching mechanism has been proposed to explain all these observations (11, 38, 47).

The studies mentioned above have demonstrated that homologous crossovers occur more frequently than nonhomologous events in BMV (37). Characterization of more than 100 homologous recombinants revealed that all had crossover sites limited to long homologous regions among templates and that crossovers occurred precisely at corresponding nucleotide positions (12, 38a). In contrast, the statistical nature of the distribution of nonhomologous crossovers was observed by us at local heteroduplex regions formed between recombining BMV RNA components (38). This and the observed precision of homologous recombination suggested that a different mechanism may be operating during homologous recombination.

To understand the mechanism of homologous recombination, in this work we have investigated sequence and structural requirements of homologous recombination in BMV. A recombination system in which a 60-nt BMV RNA3 3′ noncoding sequence supports efficient homologous crossovers with corresponding wt RNA2 sequences has been developed. A set of nested deletions within this 60-nt region reveals a direct correlation between the length of sequence identity and recombination frequency. Besides length, the extent of sequence homology influenced both recombination incidence and the distribution of crossover sites. Nearly 20% of homologous recombinants were imprecise since they contained either nucleotide mismatches, small deletions, or small insertions within the region of crossovers. We discuss our results in relation to possible mechanisms of homologous recombination.

MATERIALS AND METHODS

Materials. Plasmids pB1TP3, pB2TP5, and pB3TP7 (23) were used to synthesize in vitro-transcribed wt BMV RNA components 1, 2, and 3, respectively. Moloney murine leukemia virus reverse transcriptase, restriction enzymes, and T7 RNA polymerase were from Gibco BRL (Gaithersburg, Md.), and the Sequenase kit was from U.S. Biochemicals (Cleveland, Ohio). The following oligonucleotide primers were used in this study (unique *Eco*RI and *Bam*HI sites are underlined, and alternative bases are shown in parentheses): 1, 5′-CAGT GAATTCTGGTCTCTTTTAGAGATTTACAG-3′; 2, 5′-CTGAAGCAGTGC CTGCTAAGGCGGTC-3′; 27, 5′-CAGTGGATCCAAGTGTCCTACCTGGA CAGG-3′; 28, 5′-CAGTGGATCCGCCAAAGTGTCCTACCTGGAC-3′; 48, 5′-CAGTGGATCCTACCTGGACAGGGTCTC-3′; 49, 5′-CAGTGGATCCA GTGTCCTACCTGGACAGG-3′; 52, 5′-CAGTGGATCCATTGTAC(TC)GA (TC)TCAA(CG)AAGCTTTTAACCTTAGCC(AT)AAGTGTCCTACCT-3′; 114, 5′-CAGTGGATCCAACTCGAGCACAACGAAGGCTG-3′; 115, 5′-CA GTGGATCCGTCAACCACGAC(TG)A(TG)CAG(TG)TA(TG)TG(TG)AC (TG)GAT(TC)CAACAAGCTTTTAACCT-3′; 116, 5′-CAGTGGATCCGTCA ACCACGAC(TC)A(TC)CAG(TC)TA(TC)TG(TC)AC(TC)GAT(TC) CAACAAGCTTTTAACCT-3′; 166, 5′-CAGTGGATCCTTAG(GC)CAAAGT GTCCTAC-3′; 178, 5′-CAGTGAATTCTTTCGACTAGGCGCTGCCCACCA-3′.

Plasmid construction. PN100 and PN-H series plasmids (described below) are derivatives of pB3TP7, from which infectious wt BMV RNA3 can be synthesized in vitro (23). To construct plasmid PN100 (Fig. 1A), the following multistep approach was used. First, plasmid PN100A-C was generated as follows. A 765-bp 3′ cDNA fragment derived from pCC3TP4, a plasmid containing full-length cDNA of RNA3 of cowpea chlorotic mottle virus (3), was amplified by PCR with primers 114 and 178 (Fig. 1A). The amplified cDNA fragment was digested with *Spe*I restriction enzyme, and the resulting 555-bp cDNA fragment (representing the 5′ portion of region C [Fig. 1A]) was ligated to *Spe*I-linearized PN0, containing regions A and B as well as the 3′ part of region C (38). After ligation, a new round of PCR was used to amplify the whole sequence of regions A to C with primers 1 and 114. The resulting 1.1-kb PCR fragment was purified by low-melting-point agarose gel electrophoresis (49) followed by digestion of the ends with *Bam*HI and *Eco*RI. The digested PCR fragment was then used to replace the 3′ 240-bp *Bam*HI-*Eco*RI fragment of pB3TP7B (a plasmid containing the full-length cDNA of BMV RNA3 with a *Bam*HI linker mutation at a *Tth*111I site, position 234 as counted from the 3′ end according to Ahlquist et al. [2]). The resulting plasmid, PN100A-C, contained regions A to C (shown as part of PN100 in Fig. 1A) and a unique *Bam*HI site immediately upstream of region C. To obtain PN100, a 158-bp cDNA fragment representing the upstream portion of the 3′ end of BMV RNA3 (including region D [Fig. 1A]) was amplified from the pB3TP7 template by PCR with primers 2 and 48. The resulting cDNA fragment was digested with *Bam*HI and *Xba*I and then ligated to the corresponding sites in PN100A-C. The 3′ noncoding region of PN100 RNA3 was 1,233 nt in length (Fig. 1A). Region A contained RNA3 sequences between positions 1 and 162 (nucleotide numbering is from the 3′ end of wt RNA throughout this work) and an upstream RNA1-derived region (positions 163 to 236 on wt RNA1). Region B contained RNA3 sequences between positions 7 and 200. Both region A and region B contained an m4 deletion (positions 81 to 100 on wt RNA3). Region C consisted of 765 nt derived from cowpea chlorotic mottle virus RNA3 (positions 24 to 788). Region D contained RNA3 sequences between positions 220 and 297 on wt RNA3.

To generate the constructs depicted in Fig. 2B, the upstream part of the 3′ sequence of pB3TP7 (positions 160 to 392, which included regions R and D as well as the 3′ end of the coat protein open reading frame) was amplified with primer 2 and either primer 115 or 116 (Fig. 1A). The resulting PCR fragments were digested with *Bam*HI and *Xba*I and ligated into PN100 at corresponding sites. Since primers 115 and 116 were expected to introduce A-to-C and A-to-G mismatch mutations, respectively, at several positions within region R, the entire amplified region was sequenced to confirm the presence of mutations. The actual region R sequences of selected constructs are shown in Fig. 2B. The plasmid that did not contain any mutations in region R (it had sequences representing wt RNA3) was designated PN-H26 (Fig. 1A).

Constructs PN-H52, PN-H166, PN-H28, PN-H27, and PN-H49 (Fig. 2A) were obtained by using similar PCR-based technology. The 5′ portions of region R and the entire region D in PN-H26 (Fig. 1A) were amplified by PCR with pairs consisting of 5′ primer 2 and one of the following 3′ primers: 52, 166, 28, 27, and 49, respectively. PCR products were digested with *Bam*HI and *Xba*I and used to replace the corresponding fragment in PN100. Constructs PN-H65 and PN-H66 (Fig. 2A) were obtained by digestion of constructs PN-H26 and PN-H54 (a point mutation derivative of PN-H52) (not shown) with *Hin*dIII and *Hin*cII (both sites were located within region R), T4 DNA polymerase treatment, and recircularization. The entire PCR-amplified region was sequenced to confirm the mutations introduced in all of the constructs described above.

Plant inoculations. Leaves of *Chenopodium quinoa*, a local lesion host for BMV (33a), were inoculated with a mixture of transcribed BMV RNA components, as described by Nagy and Bujarski (38). Briefly, a mixture of 1 μg of each transcript in 15 μl of inoculation buffer (10 mM Tris [pH 8.0], 1 mM EDTA, 0.1% celite, 0.1% bentonite) was used to inoculate one fully expanded leaf. Six leaves were inoculated for each RNA3 mutant. Each experiment was repeated twice.

RT-PCR amplifications, cloning, and sequencing. Total RNA was isolated from separate local lesions and used for reverse transcription PCR (RT-PCR) amplification, exactly as described previously (37). The 3′ end of progeny RNA3 was amplified by using primers 1 and 2 (Fig. 1A). Standard 1.5% agarose gel electrophoresis was used to estimate the sizes of cDNA products (49). cDNA fragments were digested with *Eco*RI and *Xba*I restriction enzymes and ligated between these sites into the pGEM3 zf(−) cloning vector (Promega). Sites of crossovers were determined by sequencing according to the manufacturer's specifications (U.S. Biochemicals).

RESULTS

A 60-nt region of identity supports homologous crossovers between RNAs 2 and 3. In vivo accumulation of homologous BMV RNA3 recombinants containing crossovers either within or upstream of the promoter for minus-strand RNA synthesis has been described previously (9, 37, 46, 47). A 60-nt upstream portion of 3′ noncoding sequences was of special interest because previous studies revealed that this segment can be altered without debilitating RNA3 replication (32). Therefore, this region, which is homologous between RNAs 2 and 3, was selected for further studies.

An RNA3-based recombination vector that replicated inefficiently in *C. quinoa* was engineered. This vector, PN100, was similar to a published construct (PN0) used as a vector for nonhomologous recombination (38). As illustrated in Fig. 1A, the 3′ noncoding region of PN100 is much longer than that of wt RNA3. Its excessive length (1,233 nt) as well as the presence

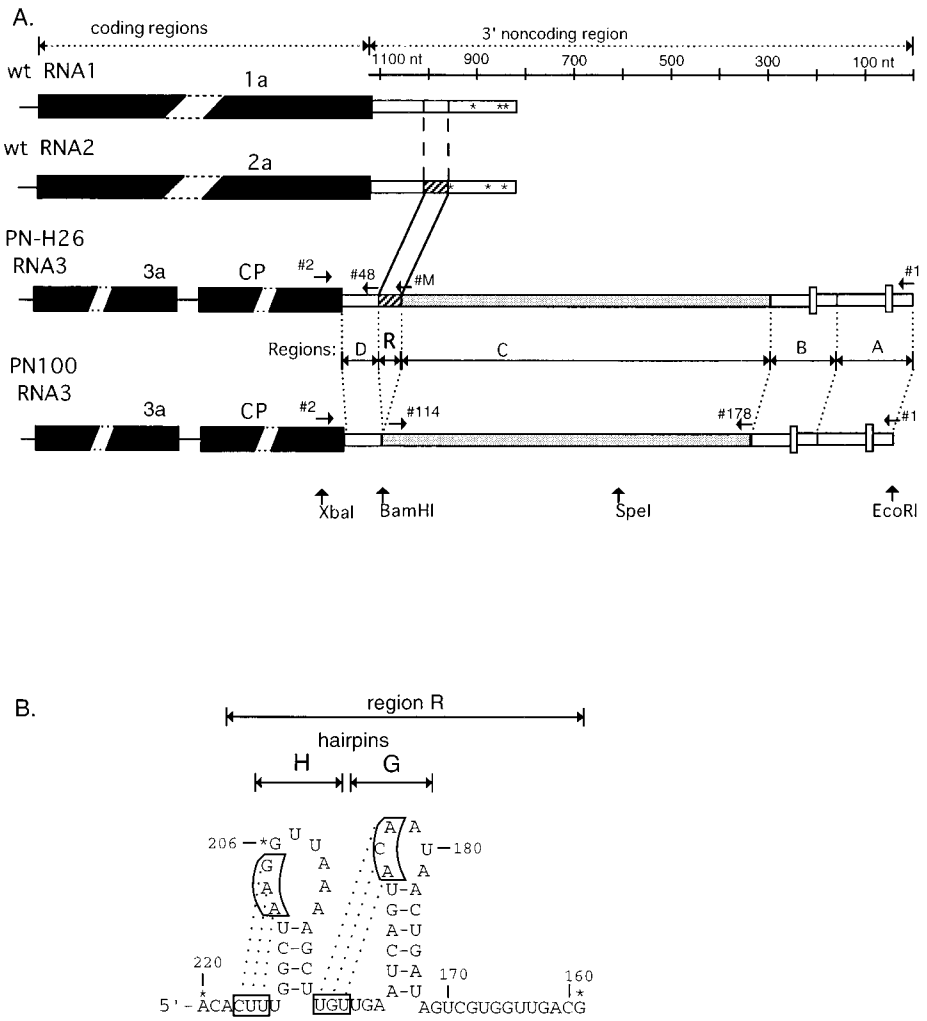

FIG. 1. (A) Schematic representation of the 3′ noncoding region of wt BMV RNAs 1 and 2 and PN-H26 and PN100 RNA3 constructs. The PN100 RNA3 mutant contains a defective 3′ noncoding region that consists of four 3′ noncoding sequence elements shown by horizontal double-headed arrows (regions A to D; described in Materials and Methods). The locations of two viable m4 deletions are shown by small rectangular boxes. PN-H26 RNA3, a derivative of PN100, contains a 60-nt RNA3-derived sequence (region R, positions 160 to 219 of wt RNA3 as counted from the 3′ end) inserted in sense orientation between regions C and D of PN100. The sequence of region R in PN-H26 is identical to the corresponding RNA2 sequence (enclosed by solid lines), except at position 206. This sequence is less similar to that in RNA1 (enclosed by broken lines). The locations of restriction enzyme sites are depicted by vertical arrows, while oligonucleotide primers used for PCR are shown by short horizontal arrows above the constructs. Primer M depicts the positions of the following mutagenesis oligodeoxynucleotides: 27, 28, 49, 52, 115, 116, and 166 (see Materials and Methods). Asterisks depict the positions of those nucleotides that were different in RNAs 1, 2, and 3 and thus served as natural marker mutations. (B) Computer-predicted secondary structure of the 60-nt region R in PN-H26. Nucleotide numbers correspond to wt RNA3 sequences (positions 160 to 219 as counted from the 3′ end). The boxed nucleotides within the two hairpins, connected by dotted lines, indicate two putative pseudoknot structures that correspond to hairpins H and G in wt RNA3, as proposed by Lahser et al. (32). Asterisks depict marker mutations that are different in PN-H26 and wt RNA2.

of two m4 deletions caused PN100 RNA3 to accumulate poorly in *C. quinoa* (15% of that of wt BMV RNA3). This was expected to give a selective advantage for the accumulation of recombinant progeny (37, 38). When tested with *C. quinoa*, PN100 was relatively stable: only 11% of the local lesions examined accumulated nonhomologous recombinants with RNAs 1 or 2, with junction sites in region D of PN100 RNA3 (data not shown). RNA3 recombinants with crossovers located close to the 3′ end of RNA3 were not detected probably because of the low-level competitiveness of resulting recombinants with an extended 3′ noncoding region.

To test the activity of the 60-nt 3′ noncoding sequence in homologous recombination, the corresponding fragment was inserted into PN100 in positive-sense orientation at the unique *Bam*HI site (Fig. 1A). The sequence of this insert differed from the corresponding wt RNA2 region only at position 206 (U-to-G substitution). This established a region of local sequence identity between 3′ sequences of wt RNA2 and the resulting PN-H26 RNA3 (Fig. 1A). After coinoculation of PN-H26 with wt RNAs 1 and 2 on the leaves of *C. quinoa*, the accumulation of recombinants in induced local lesions was monitored by RT-PCR with primers 1 and 2 (Fig. 1A) as described in Materials and Methods. On the basis of the lengths of amplified cDNA products, we estimated that 90% of local lesions accumulated wt size RNA3 progeny (Fig. 2A). In local lesions, wt size RNA3 recombinants completely outgrew parental PN-H26 RNA3 molecules, demonstrating their high-level competitiveness. This finding was in agreement with our previous observations that wt size RNA3s or close to wt size RNA3s have superior competitiveness over m4-containing parental RNA3s (37, 38).

Sequencing cloned PCR products confirmed that RNA3

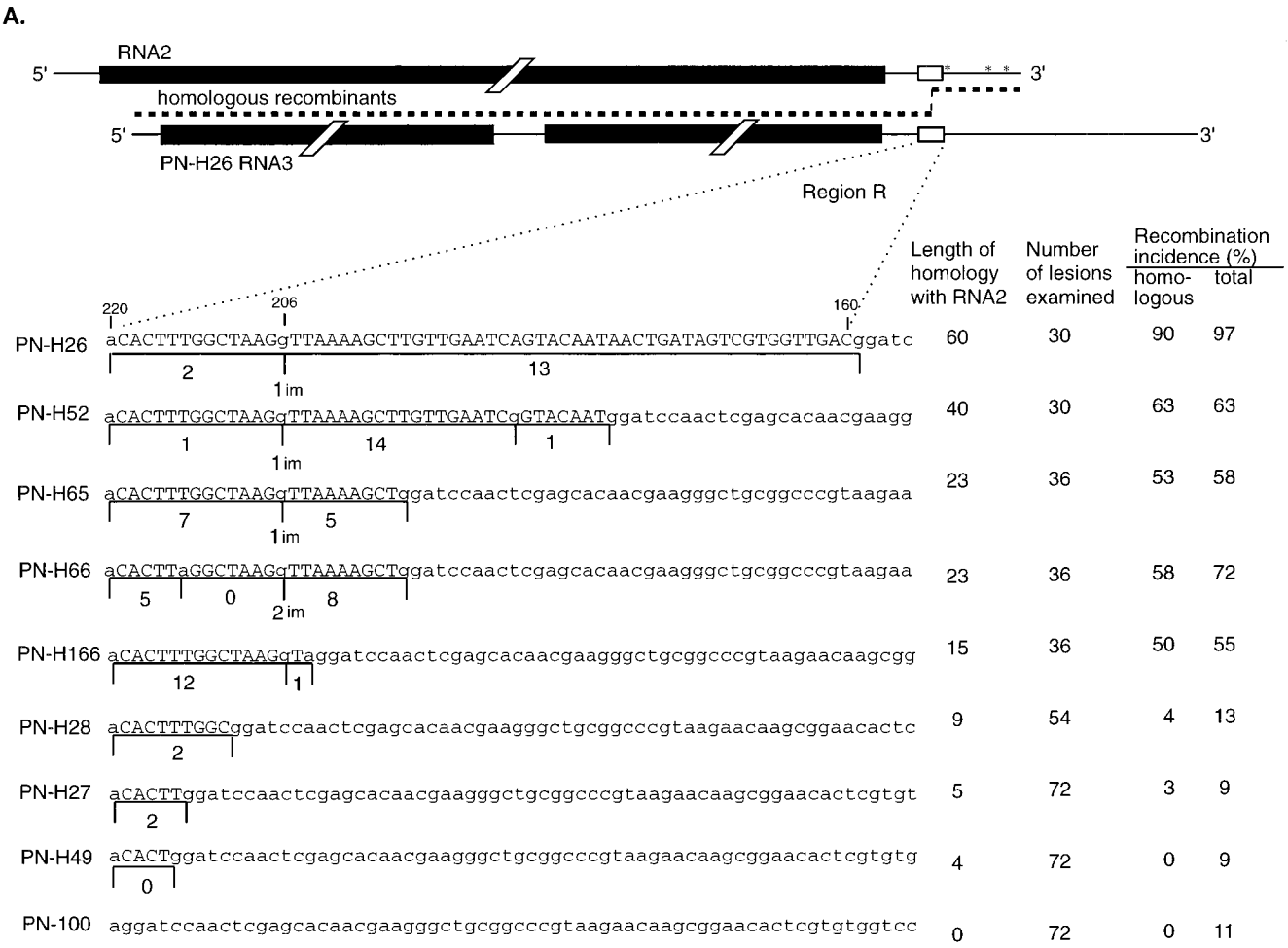

FIG. 2. Distribution of RNA2-RNA3 homologous crossover sites within the homologous sequence of region R and the incidence of total recombination and homologous recombination for nested 3′ deletion derivatives of PN-H26 (A) and mismatch derivatives of PN-H26 (B). Capital letters depict nucleotides that are identical between region R sequences (underlined) of PN-H26 or its derivatives and the corresponding sequence in wt RNA2 (Fig. 1A); lowercase letters represent heterologous sequences. Nucleotides are shown left to right in 5′-to-3′ orientation. Short vertical bars below sequence lines indicate marker mutations. The number of RNA2-RNA3 homologous recombinants isolated from separate local lesions that had crossover sites between a particular pair of markers is shown below the corresponding sequence. Each entry in this figure reflects independent RNA2-RNA3 homologous recombinants derived from separate local lesions. For analysis of the distribution of crossover sites, we mapped the junction sites by sequencing similar numbers of recombinants (13 to 21 RNA2-RNA3 homologous recombinants for each construct). Therefore, the total number of RNA2-RNA3 homologous crossover sites mapped by sequencing is usually less than the number of homologous recombinants (including not only dominant RNA2-RNA3 recombinants but also infrequent RNA1-RNA3 homologous recombinants [Table 1]) isolated and characterized by RT-PCR. The incidence of homologous recombination and total (including homologous and nonhomologous recombinants) recombination, determined by agarose gel electrophoresis of RT-PCR-amplified RNA3-specific 3′ cDNA products, was defined as the percentage of separate local lesions on *C. quinoa* that accumulated recombinants. The free energy of the predicted secondary structure within region R was calculated as previously described (41, 42). im, the site and incidence of the most frequent imprecise (aberrant) homologous recombinant (recombinant H-1 [Fig. 3B]).

components acquired 3′ sequences from RNA2 (i.e., contained RNA2-specific marker mutations at positions 44, 77, and 81 to 100) through homologous crossover events within the inserted 60-nt homologous sequence. These results established that the 60-nt sequence common to wt RNA2 and PN-H26 RNA3 can support a high frequency of homologous recombination (Fig. 2A). Control RT-PCR amplifications of mixtures of in vitro-transcribed wt RNAs 1 and 2 and either PN-H26 or PN100 RNA3s generated parental-sized, but not recombinant-sized, RNA3-specific cDNA fragments. Similar controls were published previously (38), and they exclude the possibility that recombinants represent RT-PCR artifacts (data not shown).

Effect of length of homologous region on recombination. To determine the minimal length of homologous sequences to support homologous recombination between RNA2 and RNA3, various portions of the 3′ end of the homologous insert in PN-H26 were deleted. The resulting PN-H52, PN-H65, PN-H166, PN-H28, PN-H27, and PN-H49 RNA3 constructs (Fig. 2A) retained homologous sequences of 40, 23, 15, 9, 5, and 4 nt, respectively. RT-PCR analysis of progeny RNAs isolated from separate local lesions demonstrated that PN-H52 and PN-H65, which had 40- and 23-nt homologous sequences, respectively, supported homologous recombination in 63 and 53% of local lesions (Fig. 2A). A further reduction of recombination incidence to 50% was observed for construct PN-H166 (containing a 15-nt homologous sequence), whereas PN-H28 (with a 9-nt homologous insert) and PN-H27 (with a 5-nt homologous insert) recombined very infrequently (Fig. 2A). Homologous recombinants with junction sites within a 4-nt homologous region have not been found in PN-H49 infections. These data establish that constructs with longer homologous inserts recombine with higher incidence than

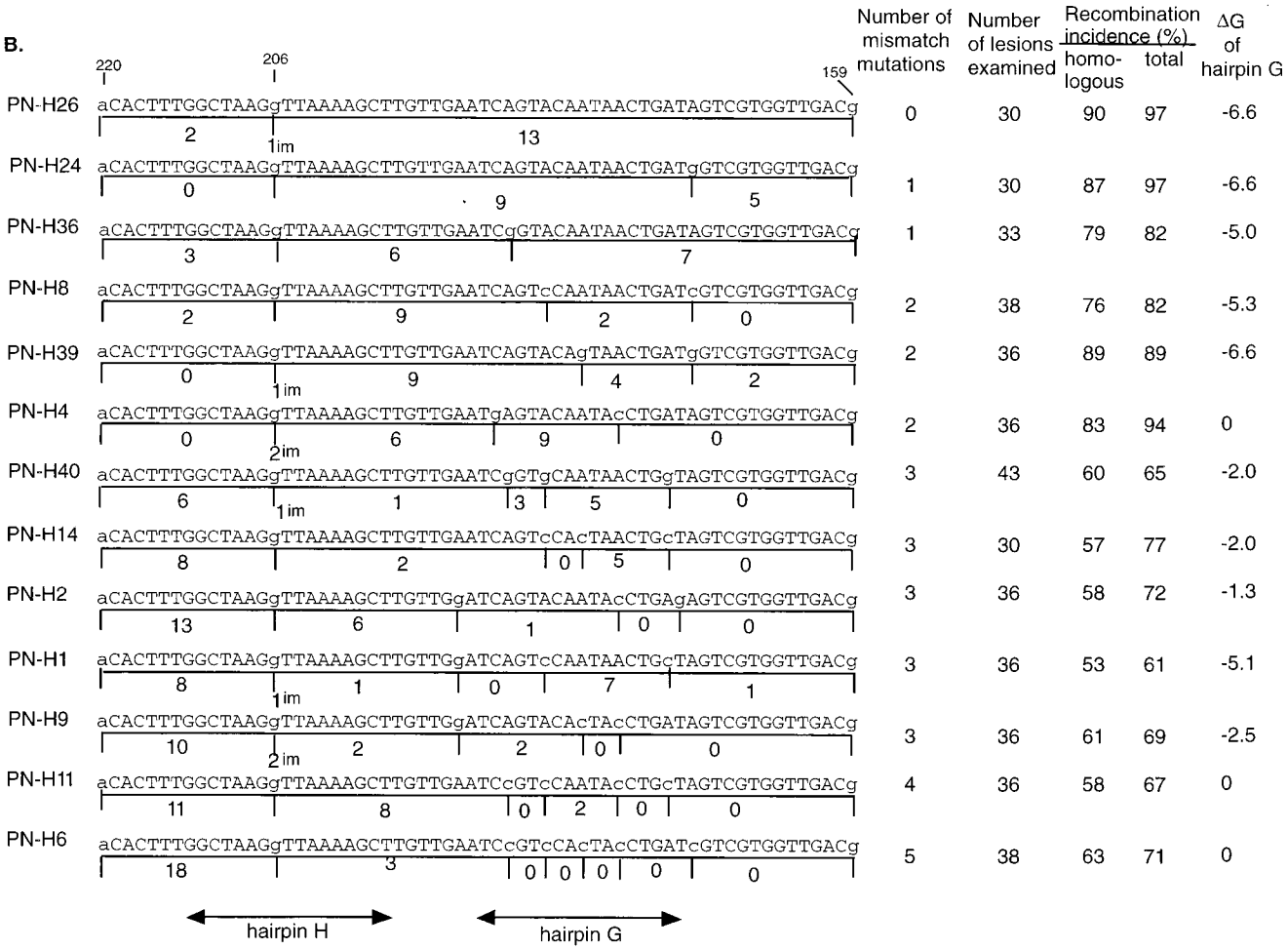

FIG. 2—*Continued.*

those with shorter inserts. Furthermore, very short (5- to 9-nt) homologous sequences can participate in homologous crossover events, though rather infrequently.

The extent of identity between homologous regions affects both recombination efficiency and the distribution of junction sites. The majority of crossovers (81%) were found to occur 3′ to the G-206 marker mutation in PN-H26-induced recombinants (Fig. 2B). To determine the effect of nucleotide mismatches on recombination, one to five point mutations were introduced 3′ to the G-206 marker into a region predicted to form a stable hairpin structure with a pseudoknot (hairpin G in Fig. 1B) (see reference 32 also). The formation of hairpin G structure in RNA3 is supported by the fact that similar pseudoknot structures have been predicted not only for the other two genomic RNAs of BMV but also among closely related bromo-, cucumo-, hordei-, and tobamovirus RNAs (32, 41, 42). Point mutations were introduced within either the stem or loop regions of hairpin G. The majority of introduced alterations were either A to C or A to G in order to disrupt or preserve (by allowing the formation of GU pairs), respectively, the double-stranded stem region and pseudoknot structure. Figure 2B shows that the presence of one or two mismatches (mutants PN-H24, PN-H36, PN-H8, PN-H39, and PN-H4) decreased the incidence of homologous recombination no more than 14% compared with that of the original PN-H26 construct. The introduction of three or more mismatches (mutants PN-H40, PN-H14, PN-H2, PN-H1, PN-H9, PN-H11, and PN-H6) decreased homologous recombination by 30 to 40%. Interestingly, the presence of three- to five-mismatch mutations in hairpin G reduced recombination incidence to a level comparable to that observed for constructs containing partial or complete deletion of hairpin G sequences (compare with constructs PN-H52, PN-H65, and PN-H66 in Fig. 2A).

These mismatch mutants were useful for more precise localization of crossover sites. As shown in Fig. 2B, one nucleotide mismatch in variants PN-H24 and PN-H36 and two mismatches in variants PN-H4, PN-H8, and PN-H39 did not markedly change the distribution of crossovers, with the majority of crosses (80 to 100%) occurring downstream of the G-206 marker mutation. In contrast, 65 and 63% of crossovers occurred upstream of the G-206 marker mutation in PN-H2 and PN-H9, three-mismatch mutants, respectively. This 5′ shift of crossovers was less obvious for the remaining three-mismatch constructs: 38, 53, and 44% of crossovers for PN-H40, PN-H14, and PN-H1, respectively, occurred upstream of the G-206 marker mutation. A clear 5′ shift of crossovers was apparent for constructs with four (PN-H11)- and five (PN-H6)-mismatch mutations, with 52 and 86% of crossovers, respectively, upstream of G-206. In total, the introduction of three or more nucleotide mismatches markedly decreased the frequency of homologous recombination in the mutated homologous region of RNA3.

TABLE 1. Percentage of homologous RNA3 recombinants resulting from crossovers with either RNA1 or RNA2

Parental RNA3 constructs	Total no. of homologous recombinants analyzed	Extent of homology (%) with[a]:		% Homologous recombinants with[b]:	
		RNA1 (positions 160 to 193)	RNA2 (positions 160 to 219)	RNA1	RNA2
PN-H26	18	88	98	0	100
PN-H24	14	85	97	0	100
PN-H36	18	91	97	6	94
PN-H8	13	82	95	0	100
PN-H39	16	82	95	0	100
PN-H4	19	82	95	5	95
PN-H40	26	91	93	35	65
PN-H14	16	79	93	6	94
PN-H2	21	79	93	5	95
PN-H1	18	79	93	0	100
PN-H9	17	79	93	6	94
PN-H11	21	76	92	5	95
PN-H6	22	73	90	5	95
Total or average[c]	213	81	94	3	97

[a] Sequence similarity of region R in RNA3 constructs to either wt RNA1 or RNA2 (within the specified positions).

[b] Determined by sequencing as described in Materials and Methods. RNA1-RNA3 and RNA2-RNA3 homologous recombinants make up the homologous recombination incidence shown in Fig. 2. Note that the source of RNA1 3′ noncoding sequences could be either a wt RNA1 component or RNA1 sequences in region A of RNA3 constructs (see Materials and Methods). In the latter case, recombinants could arise from intramolecular rearrangements (looping out) between regions R and A.

[c] For all constructs listed above except PN-H40.

There was no definitive correlation between the predicted stability of hairpin G and the distribution of crossover sites (Fig. 2B). For instance, the 6-bp stem of hairpin G was predicted to be completely destabilized by two mismatches in PN-H4 and PN-H6 and three mismatches in PN-H11, but the portion of recombinants that had crossovers within this region (downstream of the G-206 marker mutation) was 88, 14, and 48%, respectively. Also, the predicted stability of hairpin G was reduced from −6.6 to ~−2.0 kcal/mol (1 cal = 4.184 J) in PN-H40, PN-H14, and PN-H9. However, the incidence of recombination within the mutated region was 56, 47, and 25%, respectively (Fig. 2B). Taken together, these data indicate that the sequence homology between RNAs 2 and 3 was a major factor in influencing both the incidence of homologous recombination and the sites of crossovers.

Since the accumulation of particular recombinants can be influenced by postrecombinational selection (5, 37, 58), we examined whether the observed 5′ shift of crossovers resulted from selection. This was especially important because homologous recombinants with crossovers upstream of mismatch mutations would no longer contain these mismatches, while those with downstream crossovers would and the latter may not accumulate (Fig. 2B). Thus, in a control experiment, we examined whether RNA3 recombinants with five-mismatch mutations within the hairpin G region were generated and amplified to a detectable level in vivo. A mutated RNA2 molecule (designated H6-RNA2) that contained the same five-mismatch mutations in hairpin G as PN-H6 RNA3 did (Fig. 2B) was found to be infectious when coinoculated with PN-H6 RNA3 and wt RNA1. Isolated RNA3 homologous recombinants had precise crossovers with H6-RNA2 within the 60-nt homologous region and thus retained all five point mutations in hairpin G (data not shown). This confirmed that RNA3 recombinants containing the mutagenized homologous region of RNA2 are allowed to accumulate in local lesions.

A comparison of the incidence with which RNA3 mutants recombined with either RNA2 or RNA1 components and the extent of sequence identity between recombining BMV RNAs in the region of crossover further supported the role of sequence homology in homologous recombination. For instance, PN-H40 RNA3, whose sequence homology with RNA1 within the 3′ portion of its region R (91% between positions 160 and 193 [Table 1]) was almost as high as that with corresponding RNA2 sequences (93%), generated RNA1-RNA3 homologous recombinants much more frequently (35%) than the other mutants depicted in Fig. 2B. The latter were more similar to RNA2 than to RNA1. These data suggest that increasing the extent of sequence similarity increases the incidence with which homologous recombinants are isolated. Because homologous RNA2-RNA3 recombinants with crossovers within region R have been shown to be viable, this increased incidence of recombinant isolation almost certainly reflects an increased frequency of recombinogenic events.

Occurrence of point mutations, deletions, and insertions within the crossover region. Sequence analysis of 239 independently generated homologous recombinants (Fig. 2B) revealed that 33 of them (~14%) contained mismatches (nucleotide substitutions) in region R that were not present in either parental molecule (Fig. 3A). To guard against the possibility that some of these alterations represented PCR artifacts, the 60 adjacent downstream nt (positions 100 to 159, derived from wt RNA2 in RNA2-RNA3 homologous recombinants) in all the homologous recombinants generated by the constructs illustrated in Fig. 2B were sequenced. If RT-PCR was responsible for the observed mismatches, they should occur with similar frequency within the homologous and control downstream regions (27). We found that the 60-nt homologous region R contained, on average, four times more mismatches (14% of all homologous recombinants from Fig. 2B) than the 60-nt control sequence (3%). Moreover, the majority of mismatches (81%) were concentrated within actual crossover regions (flanked by a 3′ marker mutation from wt RNA2 and a 5′ marker mutation from mutated RNA3). Most mutant recombinants had single mismatches (85%); a much smaller fraction (15%) had two adjacent mismatches or two mismatches separated by one unchanged nucleotide (Fig. 3A). Another interesting feature was the nonrandom nature of mismatch mutations within the homologous region. The majority of these mutations on positive-sense RNA involved a U residue (90% of cases compared with the expected 25% if misincorporation was random) which replaced an A residue in 56%, a C residue in 20%, and a G residue in 12% of cases (Fig. 3A). Mismatch mutations in the control downstream region showed a nearly random distribution (two U-to-C substitutions, two A-to-G substitutions, two C-to-U substitutions, one U-to-A substitution, and one G-to-A substitution).

Nearly 5% of homologous recombinants contained nucleotide insertions, while 1% had deletions within the crossover region. No nucleotide insertions or deletions were observed in the control region of RNA2-RNA3 homologous recombinants. The majority of inserted nucleotides represented the repetition of one of the two flanking template nucleotides (Fig. 3B). However, some recombinants had nontemplated nucleotides (e.g., H4-3 and H9-2 [Fig. 3B]). Interestingly, two recombinants (H36-1 and H26-1) had 5 and 12 heterologous nt, respectively, of unknown origin that replaced 8 homologous nt in the crossover region. Another type of recombinant had crossover sites between heterologous nucleotides that were

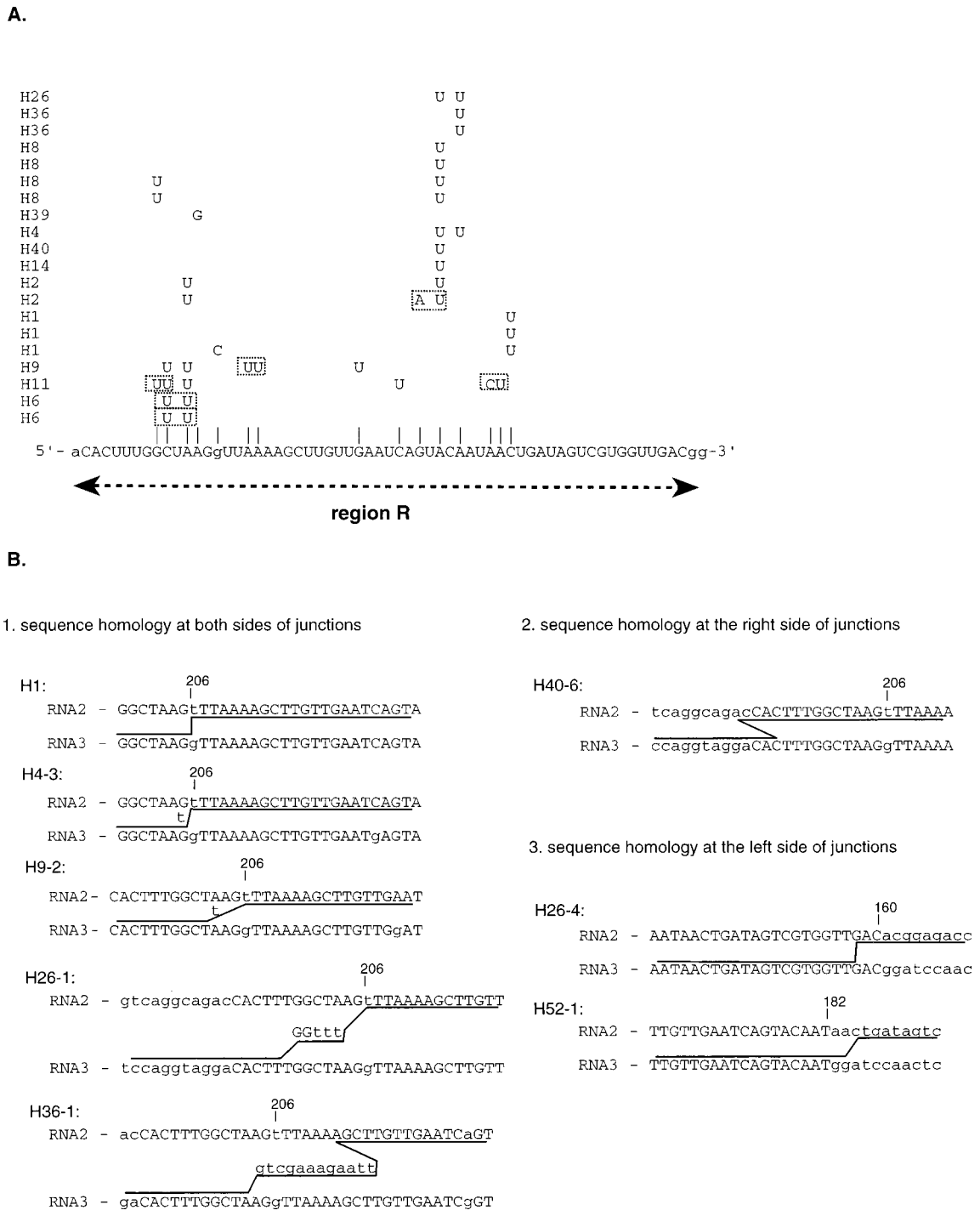

FIG. 3. Diagram summarizing the locations of single- and double-nucleotide substitutions within region R in imprecise (aberrant) homologous RNA2-RNA3 recombinants isolated from infections with constructs from Fig. 2B. Each letter represents a single-nucleotide substitution in a separate independent recombinant, even if there are multiple letters in the same line. Double-nucleotide substitutions in a recombinant are boxed by dotted lines. For simplicity, the positive-strand sequence of region R is shown only for PN-H26; sequences of region R in other constructs are shown in Fig. 2B. The names of parental RNA3 constructs are shown on the left. (B) Nucleotide sequences flanking the sites of crossovers in imprecise (aberrant) homologous RNA2-RNA3 recombinants with deletions or insertions at crossover sites. Homologous RNA2 and RNA3 sequences are shown in upper and lower lines, respectively. Capital letters depict nucleotides that are identical between mutated RNA3s and wt RNA2 (Fig. 2); lowercase letters represent mismatches. The sequences of recombinants and the sites of crossovers are depicted by solid lines inside each pair of sequences. Nontemplated nucleotides are displayed between sequences. The names of recombinants reflect their origin, except in the case of H-1. The latter recombinant was found in 12 separate local lesions induced by different RNA3 mutants (Fig. 2).

flanked, at least from one side, by long homologous sequences (e.g., recombinants H40-6 and H52-1 [Fig. 3B]).

The most frequent single nucleotide insertion, found in nearly 70% of imprecise recombinants (isolated from 12 independent infections), was a U residue at the crossover site (position 206 [or 207] of RNA2 and 207 [or 208] of RNA3; designated recombinant H-1) (Fig. 3B). Other imprecise recombinants also had deletions or insertions at or near this hot spot position (recombinants H4-3, H26-1, H9-2, and H36-1 [Fig. 3B]). Since these insertions and deletions were found exclusively within the region of crossovers (between the specific marker mutations), they must have resulted from in vivo recombination events. In control experiments, multiple independent RT-PCR amplifications were performed on total nucleic acid extracts isolated from separate local lesions of *C. quinoa*. Such RT-PCRs always reproducibly led to the isolation of a common recombinant cDNA sequence, as demonstrated by sequence analysis of cloned cDNA fragments (data not shown). The reproducible isolation of imprecise homologous recombinants from a given total nucleic acid extract, but not from other independent samples, ruled out the possibility that nontemplated nucleotides were introduced during RT-PCR rather than during BMV infection.

During this work, depending on the particular mutant combination, we found that nonhomologous recombinants were generated in 0 to 20% of local lesions (Fig. 2). Since this type of recombinant has been previously characterized in detail (9, 37, 38), nonhomologous recombinants were not included in this report.

DISCUSSION

Although homologous RNA recombination has been described for several viruses, including BMV (see the introduction), the sequence and structural requirements of homologous crossovers are not well understood. In the experiments reported here, we investigated the effects of such factors as the length of homologous sequence, the extent of sequence identity between recombining BMV RNA segments, and secondary structures at the sites of crossovers on homologous recombination. The data presented here establish that a 60-nt 3′ sequence in RNA3 can promote efficient homologous crossovers with the corresponding RNA2 region. Deletions within this homologous region revealed that constructs with longer homologous regions recombined with higher incidence than constructs with shorter ones. These data provide experimental evidence that the length of the homologous region affects RNA recombination in BMV. The observation that an identity as short as 15 nt supported efficient homologous crossovers in BMV demonstrates that homologous recombination can occur not only between long homologous regions, as observed previously for picornaviruses (28, 29), coronaviruses (35), bacteriophage Qβ (40), and bromoviruses (37, 46, 47), but also between short regions. This finding, in turn, suggests that recombination between homologous sequences might be more common than previously anticipated. Short homologous sequences can be easily found between related viral RNAs as well as unrelated viral RNAs and have been postulated to facilitate recombination between otherwise heterologous sequences in bacteriophages Qβ and ϕ6 and in tombusviruses (8, 39, 58) as well as to promote deletion events in hypovirulence-associated mycovirus, tobamoviruses, and flock house nodavirus (34, 44, 50).

In contrast to our results described above, in which homologous recombinants were generated with high frequency, PN-H27 and PN-H28 RNA3 infections accumulated RNA2-RNA3 homologous recombinants infrequently (3 to 4% incidence of homologous recombination). This can be explained by inefficient interactions between the 5- to 9-nt homologous regions of these RNA3s and that of RNA2. Alternatively, the fact that these short sequences participated in homologous recombination events could be merely accidental. Whether other short homologous sequences can support precise crossovers in BMV remains to be determined.

Besides the length of the homologous region, our data show that the extent of sequence identity between recombining RNAs is also important. Mismatch mutations in the 3′ portion of the 60-nt homologous region in RNA3 decreased recombination in the modified region and shifted crossovers to homologous sequences further upstream (Fig. 2). The relationship between high sequence homology and homologous recombination was further supported by the observation that a shift of homologous crossovers from RNA2 to RNA1 occurred when the homologous sequence in PN-H40 was altered in such a way that it became almost as similar to the corresponding region of RNA1 as to that of RNA2 (Table 1). The importance of homology in RNA recombination has also been observed for poliovirus, in which homologous recombination occurred ~100 times more frequently between homologous viral mutants than between heterologous strains that showed 85% homology (29).

In contrast to the role of sequence homology, the effect of secondary structures in RNA3 on homologous recombination was less pronounced. Destabilization of the predicted hairpin G structure by mutations within the stem and pseudoknot structures did not correlate with either recombination incidence or the distribution of crossover sites. This result is different from that observed for turnip crinkle virus, in which an appropriate secondary structure of the acceptor RNA strand determined the efficiency of aberrant homologous recombination between turnip crinkle virus satellite RNAs (13). In addition to turnip crinkle virus, Romanova et al. (48), Tolskaya et al. (53), and Makino et al. (35) proposed a role for secondary structures in promoting homologous recombination in poliovirus and coronaviruses, respectively. Our results do not preclude the involvement of secondary structures in homologous recombination. For instance, they might be important for putative donor RNA2 sequences either within, downstream, or upstream of the sites of crossovers. Further studies are required to confirm our hypotheses.

Surprisingly, nearly 20% of homologous recombinants contained either mismatch mutations (nucleotide substitutions), insertions, or deletions within the crossover region. The low incidence of such alterations outside the crossover region (mismatch mutations in ~3% of recombinants and no deletions or insertions) strongly suggests that these mutations were created during recombination events. Thus, they may represent "fingerprints," delineating actual crossover sites. This result suggests that homologous recombination might be less accurate and, in fact, might contribute to sequence variability during virus evolution to a higher extent than previously proposed (24, 25). The fact that these events were not observed in poliovirus, coronaviruses, bacteriophage Qβ, and bromoviruses (4, 25, 29, 35, 37, 40, 46, 47) may result from selection pressure; in these studies, crossovers occurred within coding regions or promoter sequences, thus enforcing the selection of precise (i.e., functional) recombinants.

The nature of these observed homologous events differs from that previously reported for heteroduplex-mediated nonhomologous crosses in BMV (38). In the latter, crossovers were distributed between noncorresponding nucleotides on only one side of the heteroduplex formed between recombining RNA substrates. The locations of nonhomologous junctions

were affected by the strength of complementary interactions within the heteroduplex (38). This suggested that the strength of hybridization between recombining RNAs, rather than the sequence itself, was important for nonhomologous recombination in BMV. In contrast, the majority of homologous crosses were precise, and in most cases, they occurred between corresponding nucleotides within a region of identity. These features strongly suggest that sequence requirements for these two types of recombination are different.

Generation of the homologous recombinants described above can be explained by the religation of broken RNA fragments. In this case, however, one would need to assume that regions of homology facilitate the breakage and/or ligation of RNA substrates. The isolation of homologous recombinants with point mutations, insertions, or deletions within the crossover region as well as the presence of nontemplated nucleotides can be better explained by a template switching mechanism. Template switching has been demonstrated for poliovirus (29) and retrovirus recombination (20, 21) and is generally favored in all the viral RNA recombination systems described so far (33), including nonhomologous recombination in BMV (38).

To explain how sequence homology brings two RNAs together and facilitates homologous crossovers, one might assume that, as with the models proposed for poliovirus (24) and coronavirus (33) homologous recombination, the BMV replicase-nascent RNA complex dissociates from the primary RNA template. This can be stimulated by, for instance, a stable secondary structure, a protein bound to the template strand, nucleotide misincorporation by the replicase into the growing nascent strand, or a single-strand break in the template. The free aborted nascent strand could reassociate at a complementary region on another template. Another possible mechanism, proposed by Jarvis and Kirkegaard (24), is that the replicase does not dissociate from the template, but it occasionally marches back on the primary template and exposes a short non-base-paired region of the nascent strand. This region could hybridize to a new acceptor strand, and then the replicase could begin copying the new template. The ability to retract on the primary template has been described for Klenow DNA-dependent DNA polymerase (16) and for human RNA polymerase II at strong pausing sites (26, 56).

Some of the imprecise (aberrant [33]) homologous recombinants observed during this work might also have been generated by such mechanisms. The only difference in producing precise or imprecise recombinants would be that, in the latter case, the very 3′ end of the nascent strand misanneals to the acceptor strand. Accordingly, the most frequent imprecise homologous crossovers occurred within a stretch of AU nucleotides (recombinants H-1, H4-3, H9-2, and H26-1 [Fig. 3B]), where misannealing might occur more easily than in GC-rich regions (in the latter case, annealing between the aborted nascent strand and the acceptor strand is energetically more stable). As an alternative to the misannealing mechanism, recombinants with insertions might have resulted from nontemplated addition of nucleotides by the viral replicase during template switching (e.g., replicase stuttering or terminal transferase activity of the replicase). This has been postulated to explain nonhomologous recombinants containing nontemplated nucleotides at the sites of crossovers (13, 38). The latter mechanism, however, cannot explain the generation of imprecise (aberrant) homologous recombinants with deletions. The 12-nt nonviral insert in recombinant H36-1 (Fig. 3B) might be of host origin. A computer search of the GenBank database revealed a perfect 11-nt match between this insert and the chloroplast sequence (ORF 321) from rice (20a).

Another mechanism of homologous recombination might involve Holliday-like structures between double-stranded BMV RNA replicative forms, similar to those operating during homologous recombination between double-stranded DNA molecules (43). However, this mechanism seems unlikely to occur in BMV since 15-nt homologous sequences probably cannot form a Holliday-like structure; the shortest homologous DNA sequence that supported low recombination efficiency was ~50 bp in length (51).

In conclusion, our study reveals the importance of such factors as the length and extent of sequence identity for homologous recombination in BMV. Since these observations are limited to a single region within the putative acceptor BMV RNA3 molecule, further experiments are required to assess the extent to which other RNA3 sequences or putative donor RNA2 sequences contribute to homologous recombination in BMV. By their contrast with the requirements for heteroduplex-mediated nonhomologous recombination, our results open new experimental opportunities toward understanding the mechanism involved and thus the clear distinction between homologous and nonhomologous recombination in not only BMV but other related RNA viruses.

ACKNOWLEDGMENTS

We thank W. Filipowicz, C. Kirkegaard, A. E. Simon, T. Hohn, and A. White for comments and discussions.

This work was supported by a grant from the National Institute for Allergy and Infectious Diseases (RO1 AI26769) and by the Plant Molecular Biology Center at Northern Illinois University.

REFERENCES

1. **Ahlquist, P.** 1992. Bromovirus RNA replication and transcription. Curr. Opin. Genet. Dev. **2:**71–76.
2. **Ahlquist, P., R. Dasgupta, and P. Kaesberg.** 1984. Nucleotide sequence of the brome mosaic virus genome and its implications for viral replication. J. Mol. Biol. **172:**369–383.
3. **Allison, R. F., M. Janda, and P. Ahlquist.** 1988. Infectious in vitro transcripts from cowpea chlorotic mottle virus cDNA clones and exchange of individual RNA components with brome mosaic virus. J. Virol. **62:**3581–3588.
4. **Allison, R. F., G. Thompson, and P. Ahlquist.** 1990. Regeneration of a functional RNA virus genome by recombination between deletion mutants and requirement for cowpea chlorotic mottle virus 3a and coat genes for systemic infection. Proc. Natl. Acad. Sci. USA **87:**1820–1824.
5. **Banner, L. R., and M. M. C. Lai.** 1991. Random nature of coronavirus recombination in the absence of selection pressure. Virology **185:**441–445.
6. **Beck, D. L., and W. O. Dawson.** 1990. Deletion of repeated sequences from tobacco mosaic virus mutants with two coat protein genes. Virology **177:**462–469.
7. **Bergmann, M., A. García-Sastre, and P. Palese.** 1992. Transfection-mediated recombination of influenza A virus. J. Virol. **66:**7576–7580.
8. **Biebricher, C. K., and R. Luce.** 1992. In vitro recombination and terminal elongation of RNA by Qβ replicase. EMBO J. **11:**5129–5135.
9. **Bujarski, J. J., and A. M. Dzianott.** 1991. Generation and analysis of nonhomologous RNA-RNA recombinants in brome mosaic virus: sequence complementarities at crossover sites. J. Virol. **65:**4153–4159.
10. **Bujarski, J. J., and P. Kaesberg.** 1986. Genetic recombination between RNA components of a multipartite plant virus. Nature (London) **321:**528–531.
11. **Bujarski, J. J., and P. D. Nagy.** 1994. Genetic RNA-RNA recombination in positive-stranded RNA viruses of plants, p. 1–24. *In* J. Paszkowski (ed.), Homologous recombination in plants. Kluwer Academic Publisher, Dordrecht, The Netherlands.
12. **Bujarski, J. J., P. D. Nagy, and S. Flasinski.** 1994. Molecular studies of genetic RNA-RNA recombination in brome mosaic virus. Adv. Virus Res. **43:**275–302.
13. **Cascone, P. J., C. D. Carpenter, X. H. Li, and A. E. Simon.** 1990. Recombination between satellite RNAs of turnip crinkle virus. EMBO J. **9:**1709–1715.
14. **Cascone, P. J., T. F. Haydar, and A. E. Simon.** 1993. Sequences and structures required for recombination between virus-associated RNAs. Science **260:**801–805.
15. **Dolja, V. V., and J. C. Carrington.** 1992. Evolution of positive-strand RNA viruses. Semin. Virol. **3:**315–326.

16. **Freemont, P. S., J. M. Friedman, L. S. Beese, M. R. Sanderson, and T. A. Steitz.** 1988. Cocrystal structure of an editing complex of Klenow fragment with DNA. Proc. Natl. Acad. Sci. USA **85:**8924–8929.
17. **Gibbs, A.** 1987. A molecular evolution of viruses: "trees," "clocks," and "modules." J. Cell Sci. **7**(Suppl.)**:**319–337.
18. **Goldbach, R.** 1990. Genome similarities between positive-strand RNA viruses from plants and animals, p. 3–11. *In* M. A. Brinton and F. X. Heinz (ed.), New aspects of positive-strand RNA viruses. American Society for Microbiology, Washington, D.C.
19. **Goldbach, R., O. Le Gall, and J. Wellink.** 1991. Alpha-like viruses in plants. Semin. Virol. **2:**19–25.
20. **Goodrich, D. W., and P. H. Duesberg.** 1990. Retroviral recombination during reverse transcription. Proc. Natl. Acad. Sci. USA **87:**2052–2056.
20a. **Hiratsuka, J., H. Shimada, R. Whittier, T. Ishibashi, M. Sakamoto, M. Mori, C. Kondo, Y. Honji, C. R. Sun, B. Y. Meng, Y. Q. Li, A. Kanno, Y. Nishizawa, A. Hirai, K. Shinozaki, and M. Sugiura.** 1989. The complete sequence of the rice (*Oryza sativa*) chloroplast genome: intermolecular recombination between distinct tRNA genes accounts for a major plastid DNA inversion during the evolution of cereals. Mol. Gen. Genet. **217:**185–194.
21. **Hu, W.-S., and H. M. Temin.** 1990. Retroviral recombination and reverse transcription. Science **250:**1227–1233.
22. **Ishikawa, M., P. Kroner, P. Ahlquist, and T. Meshi.** 1991. Biological activities of hybrid RNAs generated by 3′-end exchanges between tobacco mosaic and brome mosaic viruses. J. Virol. **65:**3451–3459.
23. **Janda, M., R. French, and P. Ahlquist.** 1987. High efficiency T7 polymerase synthesis of infectious RNA from cloned brome mosaic virus cDNA and effects of 5′ extensions of transcript infectivity. Virology **158:**259–262.
24. **Jarvis, T. C., and K. Kirkegaard.** 1991. The polymerase in its labyrinth: mechanisms and implications of RNA recombination. Trends Genet. **7:**186–191.
25. **Jarvis, T. C., and K. Kirkegaard.** 1992. Poliovirus RNA recombination: mechanistic studies in the absence of selection. EMBO J. **11:**3135–3145.
26. **Kassavetis, G. A., and E. P. Geiduschek.** 1993. RNA polymerase marching backward. Science **259:**944–945.
27. **Kearney, C. M., J. Donson, G. E. Jones, and W. O. Dawson.** 1993. Low level of genetic drift in foreign sequences replicating in an RNA virus in plants. Virology **192:**11–17.
28. **King, A. M. Q.** 1988. Genetic recombination in positive strand RNA viruses, p. 149–185. *In* E. Domingo, J. J. Holland, and P. Ahlquist (ed.), RNA genetics, vol. II. CRC Press, Inc., Boca Raton, Fla.
29. **Kirkegaard, K., and D. Baltimore.** 1986. The mechanism of RNA recombination in poliovirus. Cell **47:**433–443.
30. **Koetzner, C. A., M. M. Parker, C. S. Ricard, L. S. Sturman, and P. S. Masters.** 1992. Repair and mutagenesis of the genome of a deletion mutant of the coronavirus mouse hepatitis virus by targeted RNA recombination. J. Virol. **66:**1841–1848.
31. **Kuge, S., I. Saito, and A. Nomoto.** 1986. Primary structure of poliovirus defective-interfering particule genomes and possible generation mechanisms of the particules. J. Mol. Biol. **192:**473–487.
32. **Lahser, F. C., L. E. Marsh, and T. C. Hall.** 1993. Contributions of the brome mosaic virus RNA-3 3′-nontranslated region to replication and translation. J. Virol. **67:**3295–3303.
33. **Lai, M. C. M.** 1992. RNA recombination in animal and plant viruses. Microbiol. Rev. **56:**61–79.
33a. **Lane, L. C.** 1977. Brome mosaic virus. CMI/AAB descriptions of plant viruses. No. 180. Commonwealth Agricultural Bureaux, Farnham Royal, Slough, England.
34. **Li, Y., and L. A. Ball.** 1993. Nonhomologous RNA recombination during negative-strand synthesis of flock house virus RNA. J. Virol. **67:**3854–3860.
35. **Makino, S., J. G. Keck, S. A. Stohlman, and M. M. C. Lai.** 1986. High-frequency RNA recombination of murine coronaviruses. J. Virol. **57:**729–737.
36. **Marsh, L. E., G. P. Pogue, C. C. Huntley, and T. C. Hall.** 1991. Insight to replication strategies and evolution of (+) strand RNA viruses provided by brome mosaic virus. Oxf. Surv. Plant Mol. Cell. Biol. **7:**297–334.
37. **Nagy, P. D., and J. J. Bujarski.** 1992. Genetic recombination in brome mosaic virus: effect of sequence and replication of RNA on accumulation of recombinants. J. Virol. **66:**6824–6828.
38. **Nagy, P. D., and J. J. Bujarski.** 1993. Targeting the site of RNA-RNA recombination in brome mosaic virus with antisense sequences. Proc. Natl. Acad. Sci. USA **90:**6390–6394.
38a. **Nagy, P. D., and J. J. Bujarski.** Unpublished data.
39. **Onodera, S., X. Qiao, P. Gottlieb, J. Strassman, M. Frilander, and L. Mindich.** 1993. RNA structure and heterologous recombination in the double-stranded RNA bacteriophage ϕ6. J. Virol. **67:**4914–4922.
40. **Palasingam, K., and P. N. Shaklee.** 1992. Reversion of Qβ RNA phage mutants by homologous RNA recombination. J. Virol. **66:**2435–2442.
41. **Pleij, C. W. A.** 1990. Pseudoknots: a new motif in the RNA game. Trends Biochem. Sci. **15:**143–147.
42. **Pleij, C. W. A., J. P. Abrahams, A. Van Belkum, K. Rietveld, and L. Bosch.** 1987. The spatial folding of the 3′ noncoding region of amynoacylatable plant viral RNAs, p. 299–316. *In* M. Brinton and R. Rueckert (ed.), Positive strand RNA viruses. Alan R. Liss, Inc., New York.
43. **Potter, H., and D. Dressler.** 1988. Genetic recombination: molecular biology, biochemistry, and evolution, p. 217–282. *In* K. B. Low (ed.), The recombination of genetic material. Academic Press, San Diego, Calif.
44. **Raffo, A. J., and W. O. Dawson.** 1991. Construction of tobacco mosaic virus subgenomic replicons that are replicated and spread systemically in tobacco plants. Virology **184:**277–289.
45. **Rao, A. L. N., and T. C. Hall.** 1990. Requirement for a viral *trans*-acting factor encoded by brome mosaic virus RNA-2 provides strong selection in vivo for functional recombinants. J. Virol. **64:**2437–2441.
46. **Rao, A. L. N., and T. C. Hall.** 1993. Recombination and polymerase error facilitate restoration of infectivity in brome mosaic virus. J. Virol. **67:**969–979.
47. **Rao, A. L. N., B. P. Sullivan, and T. C. Hall.** 1990. Use of *Chenopodium hybridum* facilitates isolation of brome mosaic virus RNA recombinants. J. Gen. Virol. **71:**1403–1407.
48. **Romanova, L. I., V. M. Blinov, E. A. Tolskaya, E. G. Viktorova, M. S. Kolesnikova, E. A. Guseva, and V. I. Agol.** 1986. The primary structure of crossover regions of intertypic poliovirus recombinants: a model of recombination between RNA genomes. Virology **155:**202–213.
49. **Sambrook, J., E. F. Fritsch, and T. Maniatis.** 1989. Molecular cloning: a laboratory manual, 2nd ed. Cold Spring Harbor Laboratory, Cold Spring Harbor, N.Y.
50. **Shapira, R., G. H. Choi, B. I. Hillman, and D. L. Nuss.** 1991. The contribution of defective RNAs to the complexity of viral-encoded double-stranded RNA populations present in hypovirulent strains of the chestnut blight fungus *Cryphonectria parasitica*. EMBO J. **10:**741–746.
51. **Singer, B. S., L. Gold, P. Gauss, and D. H. Doherty.** 1982. Determination of the amount of homology required for recombination in bacteriophage T4. Cell **31:**25–33.
52. **Strauss, J. H., and E. G. Strauss.** 1988. Evolution of RNA viruses. Annu. Rev. Microbiol. **42:**657–683.
53. **Tolskaya, E. A., L. I. Romanova, V. M. Blinov, E. G. Viktorova, A. N. Sinyakov, M. S. Kolesnikova, and V. I. Agol.** 1987. Studies on the recombination between RNA genomes of poliovirus: the primary structure and nonrandom distribution of crossover regions in the genomes of intertypic poliovirus recombinants. Virology **161:**54–61.
54. **Van der Kuyl, A. C., L. Neeleman, and J. F. Bol.** 1991. Complementation and recombination between alfalfa mosaic virus RNA3 mutants in tobacco plants. Virology **183:**731–738.
55. **Van der Most, R. G., L. Heijnen, W. J. M. Spaan, and R. J. deGroot.** 1992. Homologous RNA recombination allows efficient introduction of site-specific mutations into the genome of coronavirus MHV-A59 via synthetic co-replicating RNAs. Nucleic Acids Res. **20:**3375–3381.
56. **Wang, D., and D. K. Hawley.** 1993. Identification of a 3′-5′ exonuclease activity associated with human RNA polymerase II. Proc. Natl. Acad. Sci. USA **90:**843–847.
57. **Weiss, B. G., and S. Schlesinger.** 1991. Recombination between Sindbis virus RNAs. J. Virol. **65:**4017–4025.
58. **White, K. A., and T. J. Morris.** 1994. Nonhomologous RNA recombination in tombusviruses: generation and evolution of defective interfering RNAs by stepwise deletions. J. Virol. **68:**14–24.
59. **Zimmern, D.** 1988. Evolution of RNA viruses, p. 211–240. *In* J. J. Holland, E. Domingo, and P. Ahlquist (ed.), RNA genetics. CRC Press, Inc., Boca Raton, Fla.